Acta Cryst. (1977). A33, 618–621

Absolute Structure Determination with Electron Microscopy

BY OMER VAN DER BIEST* AND GARETH THOMAS

Department of Materials Science and Engineering and Materials and Molecular Research Division, Lawrence Berkeley Laboratory, University of California, Berkeley, California 94720, *USA*

(*Received* 8 *November* 1976; *accepted* 28 *January* 1977)

A dynamical theory of electron diffraction, based on the Howie–Whelan equations and generalized to the non-centrosymmetric case, has been used successfully to determine the absolute configuration of the structure in ordered lithium ferrite ($LiFe_5O_8$) crystals. The ability to distinguish between the $P4_132$ and $P4_332$ space groups on a very fine scale has been demonstrated.

When the symmetry operations which constitute the space group of a structure include neither an inversion nor a reflection operation, then the structure can exist in two enantiomorphous forms: right-handed and left-handed. The presence of the two enantiomorphs coexisting within a sample can be verified in the electron microscope by imaging in dark field in a multi-beam orientation, with the electron beam parallel with a zone axis along which the crystal does not show a centre of symmetry in projection (Van der Biest & Thomas, 1975). One takes advantage here of a violation in Friedel's law (Serneels, Snykers, Delavignette, Gevers & Amelinckx, 1973) which may cause a difference in background intensity of the two structures. In this paper it will be shown that it is possible to determine uniquely the configuration of the structure, *i.e.* whether it is left or right-handed, with the results of a dynamical theory.

The material studied is lithium ferrite ($LiFe_5O_8$). All experimental observations in this paper were made on a Hitachi HU-650 microscope operating at 650 kV. The samples were discs of ordered lithium ferrite, chemically polished in hot phosphoric acid. This preparation technique does cause some etching along the boundaries between the enantiomorphs, but it yields otherwise smooth surfaces.

Thickness-fringe profiles were calculated for both structures with the Howie–Whelan equations (Howie & Whelan, 1961) generalized for the n-beam case:

$$\frac{d\psi_{\mathbf{h}}}{dz}=\pi i\sum_{\mathbf{g}\neq\mathbf{h}}\exp\left[2\pi i(s_{\mathbf{h}}-s_{\mathbf{g}})z\right]\left(\frac{U_{\mathbf{h}-\mathbf{g}}}{k_z}+i\frac{U'_{\mathbf{h}-\mathbf{g}}}{k_z}\right)\psi_{\mathbf{h}-\mathbf{g}}.$$

These equations are of the same form as those for centrosymmetric crystals. In the present case, however, $U_{\mathbf{h}-\mathbf{g}}$ and $U'_{\mathbf{h}-\mathbf{g}}$ are complex quantities with the provision that $U_{\mathbf{h}-\mathbf{g}}=U^*_{\mathbf{g}-\mathbf{h}}$, $U'_{\mathbf{h}-\mathbf{g}}=U'^*_{\mathbf{g}-\mathbf{h}}$. It was assumed that the phase factors of $U_{\mathbf{h}-\mathbf{g}}=|U_{\mathbf{h}-\mathbf{g}}|\exp(i\theta_{\mathbf{h}-\mathbf{g}})$ and $U'_{\mathbf{h}-\mathbf{g}}=|U'_{\mathbf{h}-\mathbf{g}}|\exp(i\varphi_{\mathbf{h}-\mathbf{g}})$ are the same, *i.e.* $\theta_{\mathbf{h}-\mathbf{g}}=\varphi_{\mathbf{h}-\mathbf{g}}$. $\psi_{\mathbf{h}}$ is the amplitude of beam **h**, z is the depth in the crystal; $s_{\mathbf{h}}$ is the deviation parameter of beam **h**. k_z is the component normal to the foil surface of the wave vector representing the incident wave, after correction for refraction by the mean potential in the crystal. $U_{\mathbf{h}}$ and $U'_{\mathbf{h}}$ are the Fourier components of the real and complex part of the crystal potential $V(\mathbf{r})+iW(\mathbf{r})$. The imaginary part is introduced to represent absorption processes in the crystal (Hashimoto, Howie & Whelan, 1960). The differential equations were integrated with a fourth-order modified Runge–Kutta method. Up to 61 beams were included in the calculations. The $4\bar{4}0$ reflection has the shortest two-beam extinction distance of the beams considered and this length ($\xi_{440}^{650\,\mathrm{kV}}=t_{440}$) was used to normalize the depth z.

Lithium ferrite has the spinel structure with a 3:1 mixture of iron and lithium ions on the octahedral sites. Below 750 °C, these ions take on an ordered arrangement. The structure of ordered lithium ferrite was determined by Braun (1952). It can occur in two enantiomorphous forms, $P4_132$ (right-handed screw axis) and $P4_332$ (left-handed screw axis). It has been shown that both forms coexist on a fine scale in an ordered sample (Van der Biest & Thomas, 1975). Fig. 1 shows an example. The orientation in the figure was near [332]. The black and white contrast in the dark field is due to the change in space group. In bright field no contrast is observed between the two enantiomorphous forms. Fig. 2(*a*) shows a crystal with a larger domain size. A boundary runs through the thick wedge-shaped crystal. It is clear from Fig. 2(*a*) that the black-white contrast observed in dark-field in Fig. 1 will be strongly dependent on the thickness of the crystal.

The orientation of Fig. 2 is very close to a symmetric [332] orientation. Fig. 3 shows a number of relevant thickness-fringe profiles calculated for this orientation. When performing these calculations, a choice has to be made for the values of the absorption parameters. For pure elements estimates of these values have been made by Humphreys & Hirsch (1968) and Hall & Hirsch (1965). For a complicated structure, such as lithium ferrite, estimates could still be made with the approach of Hall & Hirsch (1965), which takes into account thermal diffuse scattering of the electrons as the main absorption mechanism. This procedure could be very

* Present Address: Euratom Research Center, Petten, The Netherlands.

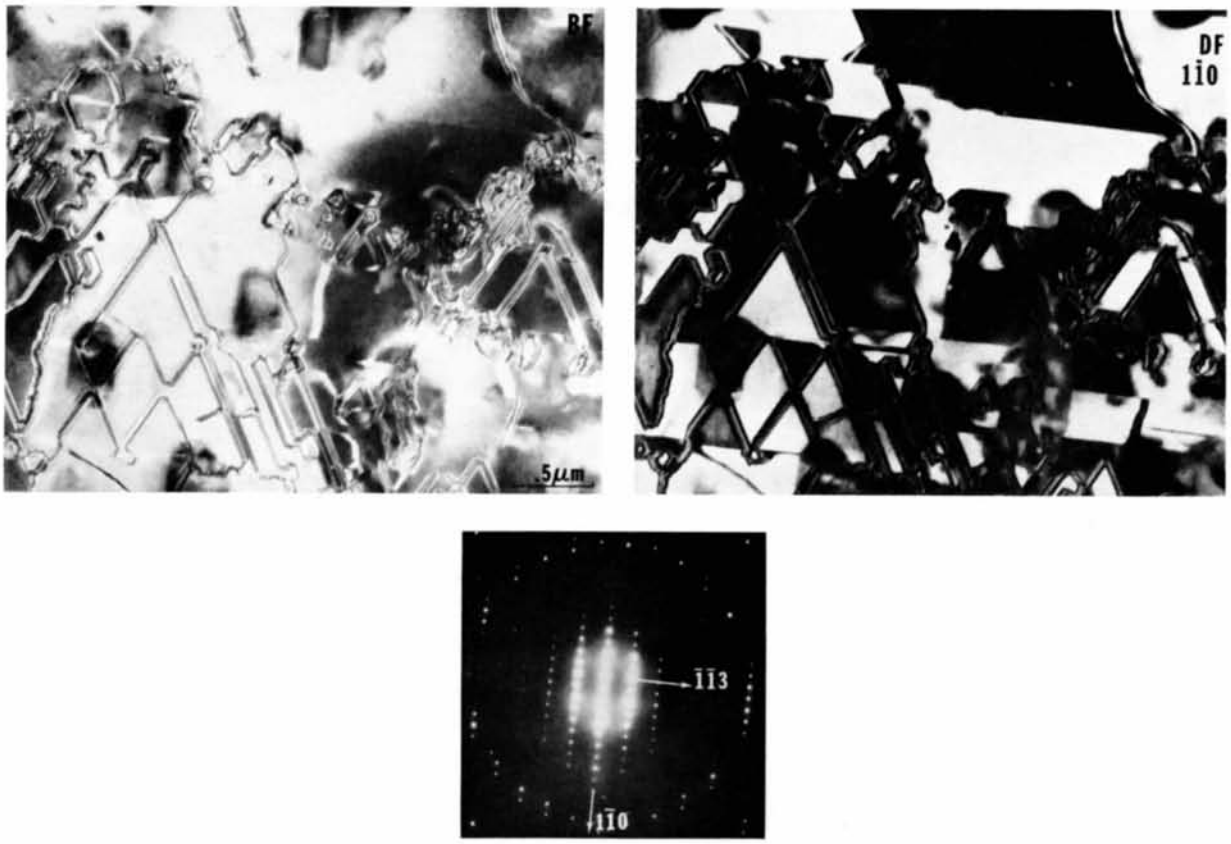

Fig. 1. Bright field (BF) and dark field (DF) ($g = 1\bar{1}0$). Symmetric orientation $[UVW] = 332$. Domains are separated by cation stacking faults. In the dark field, bright areas have the $P4_132$ structure. Dark areas have the $P4_332$ structure (for analysis, see text).

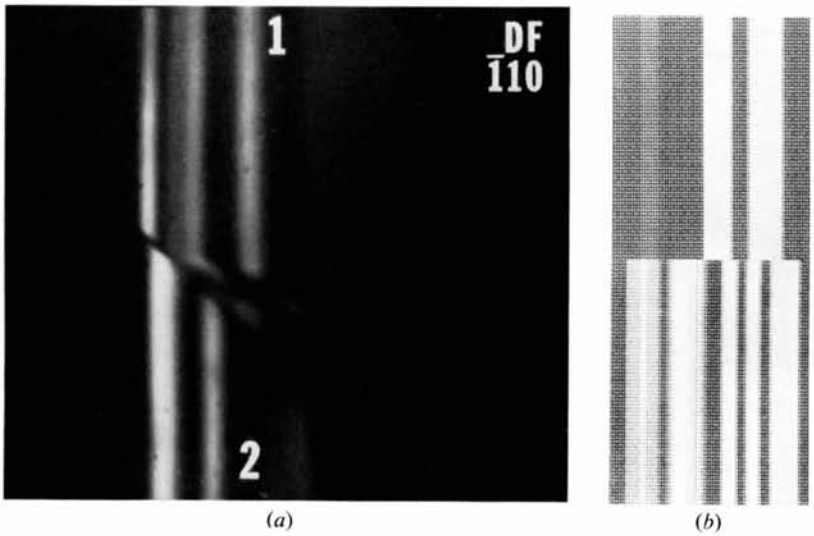

(*a*) (*b*)

Fig. 2. (*a*) Dark field ($g = 1\bar{1}0$) with corresponding diffraction pattern of a wedge-shaped crystal of lithium ferrite. The domain labelled 1 has the $P4_332$ structure. The domain labelled 2 has the $P4_132$ structure (for an analysis see text). (*b*) Simulated micrograph of (*a*). The boundary has not been simulated. $\xi_0/\xi_0' = 0{\cdot}07$ $\xi_g/\xi_g' = 0{\cdot}05$ for all g. Symmetric [332] orientation. The corresponding thickness-fringe profile is shown in Fig. 3(*b*).

[*To face p.* 618

lengthy and, in addition, the reliability of the results could be determined only through experimental measurements. These in turn are influenced by the characteristics of the instrument, contamination films on the specimen, *etc.* In order to avoid these difficulties, an empirical approach was adopted here. As will be discussed below, the value of the absorption parameters used does not influence the final result, provided that the experimental conditions are chosen judiciously. In order to simplify the problem, it was assumed throughout this study that the anomalous absorption parameters,

$$\frac{1}{\xi'_{\mathbf{g}-\mathbf{h}}}=\frac{|U'_{\mathbf{g}-\mathbf{h}}|}{k_z},$$

are the same for all beams. The thickness-fringe profiles were calculated for a range of values with the ratios ξ_g/ξ'_g and ξ_0/ξ'_0 between 0 and 0·1.

The orientation of the crystal in Fig. 1 could be deduced from the position of the Kikuchi lines on the plate. It was found that the projection of the incident wave vector **k** on the reciprocal-lattice plane (332) is very close to $k_x=(-0{\cdot}75, 1{\cdot}25, -0{\cdot}75)$. Thickness-fringe profiles for this orientation and $\mathbf{g}=1\bar{1}0$ are shown in Fig. 4. The thickness-fringe profiles for the bright field are not shown in Fig. 3 and 4 but were found to be identical for both the $P4_132$ and $P4_332$ variants, as required by the reciprocity theorem (Pogany & Turner, 1968). This provided a useful check on the performance of the computer programs. It is evident from the results in Figs. 3 and 4 that, especially in the thicker portions of the crystal, the fringe pattern is sensitive to the orientation and the values of the absorption parameters. However, it is noted (Fig. 3) that the first bright fringe will be closer to the edge of the foil in the $P4_332$ variant than in the $P4_132$ variant for $\mathbf{g}=\bar{1}10$. This result is reversed when the sign of **g** is changed (Fig. 4). This result proved to be valid for a wide range of orientations and values of the absorption parameter. The latter is understandable because near the edge of the

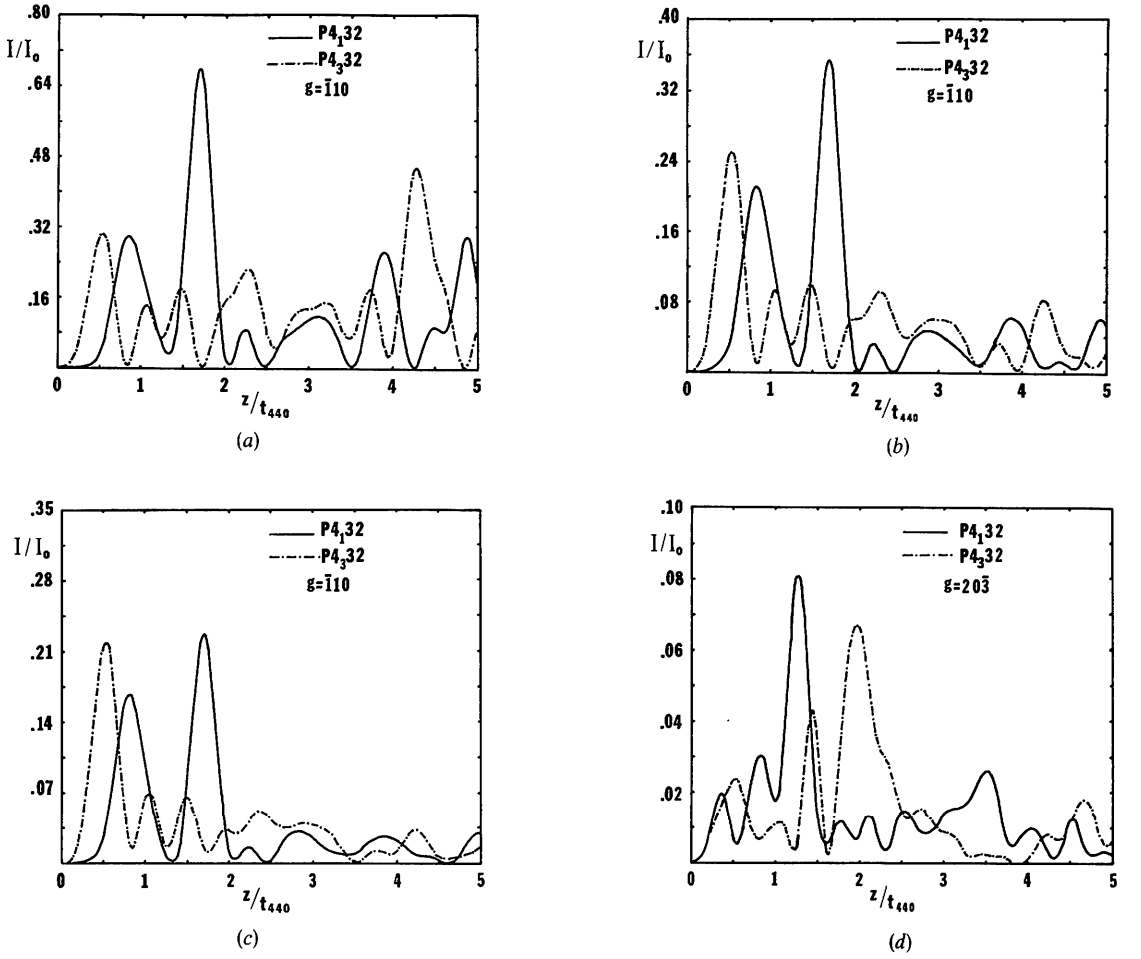

Fig. 3. Calculated thickness-fringe profiles. Voltage: 650 kV. Symmetric orientation $[UVW]=332$. 61-beam calculation $t_{440}=\xi_{440}^{650\,\mathrm{kV}}=906$ Å. All intensities start at zero at the top of the foil ($z/t=0$). (*a*) $\xi_0/\xi'_0=\xi_g/\xi'_g=0$ for all **g**; $\mathbf{g}=\bar{1}10$. (*b*) $\xi_0/\xi'_0=0{\cdot}07$ $\xi_g/\xi'_g=0{\cdot}05$ for all **g**; $\mathbf{g}=\bar{1}10$. (*c*) $\xi_0/\xi'_0=\xi_g/\xi'_g=0{\cdot}1$ for all **g**; $\mathbf{g}=\bar{1}10$. (*d*) $\xi_0/\xi'_0=0{\cdot}07$; $\xi_g/\xi'_g=0{\cdot}05$ for all **g**; $\mathbf{g}=20\bar{3}$.

foil absorption can be neglected. From this result, it is clear that in Fig. 2 domain 1 has the $P4_332$ structure and domain 2 the $P4_132$ structure. The important point from Figs. 3 and 4 is that, for $\mathbf{g}\ \langle 110\rangle$ and at the edge of the foil, the intensity for one space group increases much faster than that for the other space group, *e.g.* at $z/t_{440}=0{\cdot}15$ the intensity ratios (Fig. 3*a*) are about 10:1 for $P4_332$ compared with $P4_132$. This effect is due to the systematic multi-beam interactions.

When performing the analysis, care has to be taken to correctly index the diffraction pattern. The calculations were performed with atomic coordinates referred to right-handed axes, standard in crystallography. In the printed diffraction pattern, however, a left-handed reference system has to be used for indexing. In the general case of a non-centrosymmetric crystal, one would also need to distinguish between a $[UVW]$ orientation and $[\bar{U}\bar{V}\bar{W}]$. In the present case, this is not necessary because $[332]$ and $[\bar{3}\bar{3}\bar{2}]$ are related by a 180° rotation around the $[\bar{1}10]$ direction, which is a twofold rotation axis in both space groups. Hence, these two orientations are equivalent here. This retardation in the formation of the first bright fringe occurs only for 110-type reflections in lithium ferrite. For other reflections this does not occur (Fig. 3*d*).

An attempt was made to simulate the micrograph of Fig. 2(*a*) with the overprinting technique on the line printer of the computer. The subroutine *HALFTN*, described by Head, Humble, Clarebrough, Morton & Forwood (1973), was used for this purpose in an adapted form. A grey scale of eight steps was used by overprinting up to three different symbols. An example is shown in Fig. 2(*b*), which may be compared with Fig. 2(*a*). The boundary between the domains has not been simulated. When making this comparison, one should disregard the relative widths of the fringes as these depend only on the local slope of the crystal wedge. What is important is the way the thickness fringes meet at the boundary. Recognising the limitations of the grey scale used, which is inadequate to represent the differences in contrast in the micrograph, one may conclude that the agreement between

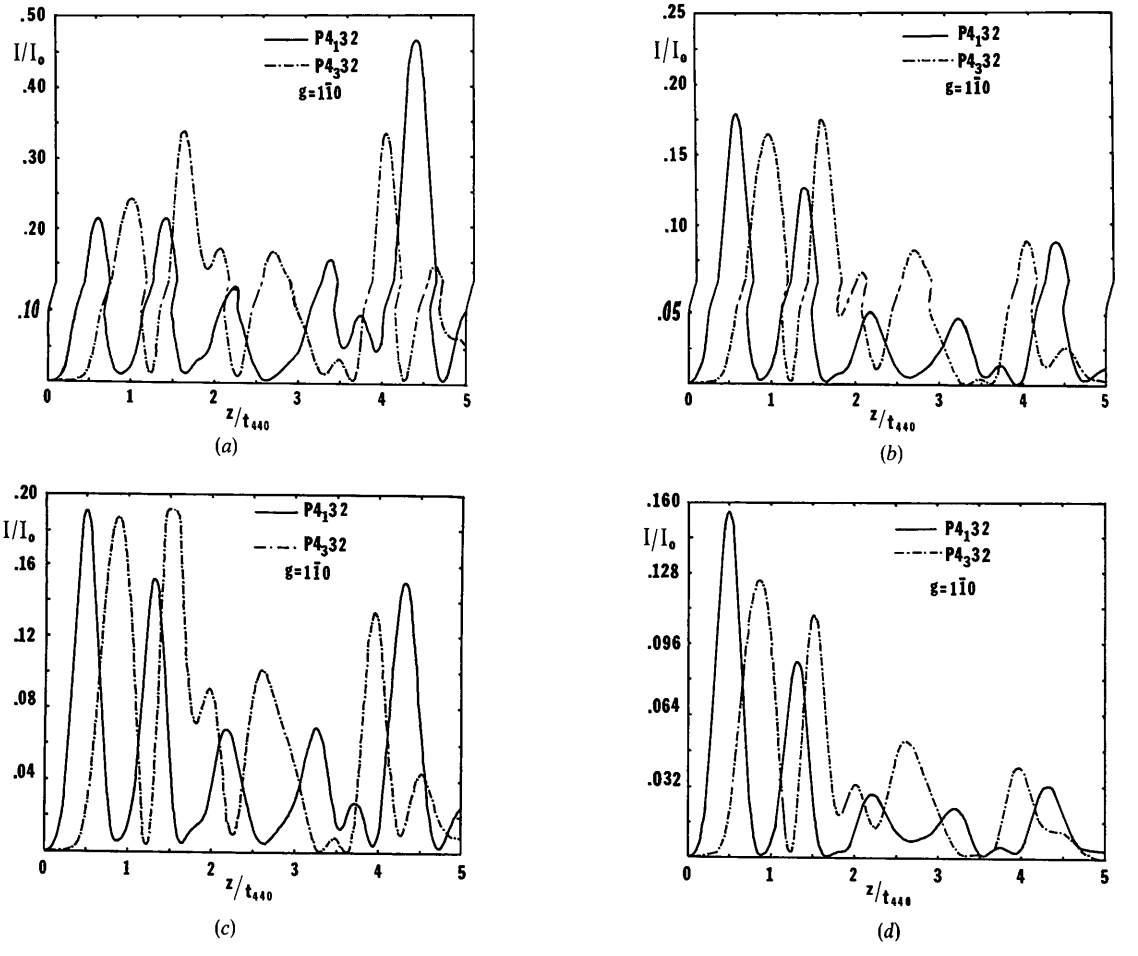

Fig. 4. Calculated thickness-fringe profiles. Orientation corresponds to that in Fig. 1, $k_x=(-175{,}0{\cdot}125,-0{\cdot}75)$ 61-beam calculation. All intensities start at zero at the top of the foil ($z/t=0$): Dark field $\mathbf{g}=1\bar{1}0$. $t_{440}=\xi_{440}^{650\,\mathrm{kV}}=906$ Å. (*a*) $\xi_0/\xi_0'=\xi_g/\xi_0'=0$ for all **g**. (*b*) $\xi_0/\xi_0'=0{\cdot}07$; $\xi_g/\xi_g'=0{\cdot}05$ for all **g**. (*c*) $\xi_0/\xi_g'=0{\cdot}05$; $\xi_g/\xi_g'=0{\cdot}03$ for all **g**. (*d*) $\xi_0/\xi_0'=\xi_g/\xi_g'=0{\cdot}1$ for all **g**.

the experimental and calculated micrographs is good.

Comparison of the simulated micrographs, calculated for a range of absorption parameters, showed that best agreement was obtained for the following values of the absorption parameters: $\xi_0/\xi'_0=0{\cdot}07$, $\xi_g/\xi'_g=0{\cdot}05$. This choice of absorption parameters is somewhat subjective, as it was found that variations in absorption parameters could be compensated for, to a limited extent, by adjusting the grey scale used. No claim is made here that these values represent an accurate determination of the absorption parameters. Still, they represent a rough guide for the values that need to be used.

The method used to determine the space group of the domains in Fig. 2, *i.e.* from the relative position of the first bright fringe, can only be used for domains ending at the edge of the crystal. In the general case, one needs to determine the thickness of the foil as accurately as possible and then deduce from the thickness-fringe profiles which variant is the brightest. The thickness of the foil in Fig. 1 has been determined accurately with a method designed by von Heimendahl (1973), who determined that the accuracy of the method is around 4% for routine work. The result for the area in Fig. 1 is 3905 Å or 4·31 ξ_{440}. Assuming an error of 5%, this yields a thickness range of 3710 to 4100 Å or 4·09 ξ_{440} to 4·53 ξ_{440}. From Fig. 4(*b*) it can be deduced that within this thickness range $P4_132$ is the brightest variant and that the largest difference occurs at 4·3 ξ_{440}. It is likely that in Fig. 1 the thickness is very close to this value, because the contrast is very pronounced.

This conclusion is not altered if other values of the absorption parameters are considered (Figs. 4*a*, *c*, *d*). A study of the points of intersection of the two thickness-fringe profiles as a function of the absorption parameters shows that these points do not depend very much on the value of the absorption parameters, although small shifts do occur. For those thicknesses where strong contrast between enantiomorphs is predicted, the value of the absorption parameter will not determine which has the stronger intensity. On the other hand, if the contrast between enantiomorphs is low, such as in the case for instance at $z=3{\cdot}5\ \xi_{440}$, for the orientation in Fig. 3, then an accurate knowledge of the absorption parameters is necessary.

The calculations yielded the following results regarding the contrast between enantiomorphous domains. (i) When only a systematic $1\bar{1}0$ row is operating, the thickness-fringe profiles of the two enantiomorphs are identical. This has been experimentally observed [see Fig. 3(*c*) in Van der Biest & Thomas (1975)]. However, a moderately strong non-systematic reflection can be sufficient to introduce contrast [Fig. 6(*c*) of Van der Biest & Thomas (1975)]. (ii) No significant difference in intensity between left and right-handed variants has been calculated for spinel-type reflections. No contrast is observed experimentally. This is understandable as the non-centrosymmetry is a direct result of the ordering process, hence the accompanying contrast phenomena such as anti-phase boundaries and contrast between enantiomorphs, will be associated with the superlattice reflections. (iii) The contrast between domains was not found for some superlattice reflections. No difference in thickness-fringe profiles as found for 112-type reflections with $[UVW]=345$ or $[UVW]=342$. This was also confirmed experimentally.

It has been shown in this paper that the dynamical theory of electron diffraction, adapted to the non-centrosymmetric case can be used successfully to determine the absolute configuration of a structure. In the general case this will require an accurate determination of the thickness of the foil as the contrast between enantiomorphs is strongly thickness dependent. It was found that if the assumption can be made that the anomalous-absorption parameter is the same for all beams, an accurate knowledge of this parameter is not necessary to make the analysis. In the particular case of lithium ferrite, the structure determination can be accomplished quickly by observing the relative location of the first fringe in domains which are terminated by the edge of the foil. This method may not be available in other structures and is in any case limited to 110-type reflections in lithium ferrite.

This report was made with support from the United States Energy Research and Development Administration. Any conclusions or opinions expressed in this report represent solely those of the authors and not necessarily those of The Regents of the University of California, the Lawrence Berkeley Laboratory or the United States Energy Research and Development Administration.

References

BRAUN, P. B. (1952). *Nature, Lond.* **170**, 1123.
HALL, C. R. & HIRSCH, P. B. (1965). *Proc. Roy. Soc.* A**286**, 158–177.
HASHIMOTO, H., HOWIE, A. & WHELAN, M. J. (1960). *Proc. Roy. Soc.* A**269**, 80–103.
HEAD, A. K., HUMBLE, P., CLAREBROUGH, L. M., MORTON, A. T., & FORWOOD, C. T. (1973). *Computed Electron Micrographs and Defect Identification.* Amsterdam: North-Holland.
HEIMENDAHL, M. VON (1973). *Micron*, **4**, 111–116.
HOWIE, A. & WHELAN, M. J. (1961). *Proc. Roy. Soc.* A**263**, 217–237.
HUMPHREYS, C. T. & HIRSCH, P. B. (1968). *Phil. Mag.* **18**, 115–122.
POGANY, A. S. & TURNER, P. S. (1968). *Acta Cryst.* A**24**, 103–109.
SERNEELS, R., SNYKERS, M., DELAVIGNETTE, P., GEVERS, R. & AMELINCKX, S. (1973). *Phys. Stat. Sol.* (*b*), **58**, 277–292.
VAN DER BIEST, O. & THOMAS, G. (1975). *Acta Cryst.* A**31**, 70–76.